

Current-driven instabilities in astrophysical jets

Linear analysis

S. Appl¹, T. Lery², and H. Baty³

¹ Institut für Angewandte Mathematik, Universität Heidelberg, Im Neuenheimer Feld 293, 69120 Heidelberg, Germany

² Department of Physics, Queen's University, Kingston, Ontario, K7L 3N6, Canada

³ Observatoire de Strasbourg, 11 rue de l'Université, 67000 Strasbourg, France

Received 19 April 1999 / Accepted 16 November 1999

Abstract. Current-driven instabilities of force-free screw pinches are studied for a large variety of magnetic configurations by means of a global linear analysis in an ideal MHD framework. The magnetic pitch, $P = rB_z/B_\phi$, in particular its value on the axis, P_0 , essentially determines the growth rate of the fastest growing kink instability and allows to identify two regimes. In the large pitch regime, representative for the majority of controlled fusion devices, the stability properties are highly sensitive to the radial pitch profile. Astrophysical jets of magnetic origin are likely to have dominantly azimuthal fields. For such configurations the properties of the fastest growing kink instability become nearly independent of the details of the pitch profile. The most unstable mode grows with an e-folding time $t_g = 7.52 P_0/v_A$ and an axial wavelength $\lambda = 8.43 P_0$ in the rest frame of the jet. The magnetic structure of jets with dominantly azimuthal fields will be modified by the fast growing kink instability. An analysis of the eigenfunction shows however that the kink is an internal mode which does not cause a significant sideways displacement of the jet surface.

Key words: instabilities – Magnetohydrodynamics (MHD) – stars: pre-main sequence – ISM: jets and outflows – galaxies: active – galaxies: jets

1. Introduction

Magnetohydrodynamic (MHD) models are favoured for the formation of jets from active galactic nuclei (AGN) and young stellar objects (YSO). Such outflows are, however, liable to magnetohydrodynamic instabilities, which may affect their propagation, or even prevent them from maintaining their integrity over hundreds of kpc or several pc, respectively. Various observed features such as wiggles, knots, and filamentary structures in extragalactic (e.g. Pearson 1996) and stellar (e.g. Reipurth & Heathcote 1997) jets may on the other hand be manifestations of instabilities of the underlying flow.

Jets of magnetic origin possess a helical field configuration. It is the azimuthal component, B_ϕ , which is equivalent to an

axial electric current, that gives rise to concern. The growth of Kelvin-Helmholtz instabilities (KHI) of supermagnetosonic jets has been shown to be reduced by the presence of the azimuthal field (Appl & Camenzind 1992). The long wavelength KH modes are, however, essentially determined by the fast magnetosonic Mach number. Similar investigations extended to the submagnetosonic regime (Appl 1996a) showed that the azimuthal field exhibits a destabilizing behaviour at small velocities. In addition to the Kelvin-Helmholtz instability, such jets are liable to current-driven instabilities (CDI), which are the subject of this paper. Great efforts have been undertaken to understand the onset and evolution of CDI in the context of controlled fusion (e.g. Bateman 1978). The CDI are also a major source of concern for magnetohydrodynamical jet models. Their role in this context has been addressed by Eichler (1993), Istomin & Pariev (1994, 1996), Appl (1996a), Spruit et al. (1997), Begelman (1998), and Lyubarskii (1999).

The situation in controlled thermonuclear reactors (CTR) differs from magnetized jets in several respects. The former are essentially static magnetic configurations, which are separated by a vacuum region from the container wall, while jets propagate at superalfvénic velocities through an ionized ambient medium. Finally, the majority of fusion machines such as the TOKAMAK, are operating in the regime where the longitudinal magnetic field is much stronger than the azimuthal field, whereas in magnetized jets both components are more likely to be at least of the same order. These differences make it difficult to directly carry over the results from fusion plasmas to astrophysical jets. The regime of a dominantly longitudinal field has been studied in detail in the context of fusion research. This is not the case for configurations with large azimuthal fields.

The purpose of this paper is the quantitative study of the linear evolution of global current-driven instabilities of astrophysical jets, to discuss the consequences for the dynamics of the outflows, and to point out the differences to fusion plasmas. To this end we start by discussing simple magnetic models for the propagating jet (Sect. 2). In Sect. 3 the linear stability analysis is described and in the next section some results from the stability of screw pinches are reviewed, to the extent they are relevant for our study. The results for relevant configurations are

Send offprint requests to: S. Appl (stefan.appl@iwr.uni-heidelberg.de)

presented in Sect. 5, followed by a careful analysis of the boundary conditions. This provides the base for the general findings which we summarize and discuss in Sect. 6. We conclude with the consequences for astrophysical jets in Sect. 7.

2. The magnetic structure

2.1. General considerations

The collimation and acceleration of these outflows is most likely of magnetic origin (Blandford & Payne 1982; e.g. Begelman et al. 1984). This mechanism eventually leads to cylindrically collimated jets (Heyvaerts & Norman 1989; Lery et al. 1999) and can produce the high Lorentz factors required by the observations. Most present 2D stationary models of the collimation and acceleration are, however, making particular assumptions, such as self-similarity (e.g. Blandford & Payne 1982), force-free magnetic fields, (e.g. Fendt et al. 1995), about the shape of the magnetic surfaces (e.g. Lery et al. 1998), or specific launching conditions (e.g. Shu et al. 1994). Given our ignorance of the details of the collimation process, and taking into account the diversity in physical conditions at the base of the jet and the surrounding medium, we consider simple jet models with a wide variety of magnetic profiles. We assume that the underlying flow is approximately stationary. The propagation of the jet through the interstellar/intergalactic medium is modeled by a sequence of quasi-equilibria, provided the ambient medium varies smoothly enough that the jet can continuously adjust itself to the changing conditions.

A magnetohydrodynamic outflow can exhibit Kelvin-Helmholtz, current-driven, and pressure-driven instabilities. In general it is not possible to unambiguously separate these effects. Only for very simple and idealized configurations one can hope for physical understanding. In this paper we restrict ourselves to current-driven modes.

For the purpose of this paper we approximate the MHD jet by an infinitely long cylindrical outflow of a perfectly conducting plasma. We suppose that the jet possesses constant density and velocity, as well as negligible thermal pressure and rotation. This excludes pressure-driven instabilities, and Kelvin-Helmholtz instabilities arise only due to the vortex sheet at the jet boundary. The equilibrium is then described by a force-free field in the rest frame of the jet,

$$\frac{dB^2}{dr} + \frac{2B_\phi^2}{r} = 0. \quad (1)$$

Cylindrical coordinates (r, z, ϕ) are used, and $B^2 = B_z^2 + B_\phi^2$. We suppose that the jet is in equilibrium with the ionized surrounding medium across its boundary at $r = R$. For the study of stability the magnetic pitch, P ,

$$P = rB_z/B_\phi. \quad (2)$$

is a crucial quantity (e.g. Bodin & Newton 1980). Consequently, we will characterize the equilibria in terms of the profile $P(r)$, which uniquely determines the magnetic field configuration.

A real jet possesses a small, but finite opening angle. Flux conservation implies that the poloidal field falls off as $1/r^2$, while

the azimuthal field scales as $1/r$, such that the latter eventually becomes dominant at large radii (Begelman et al. 1984). Parameterizing this naive scaling in terms of the total magnetic flux, Φ , of 10^{33} Gauss cm² and the total electric current, I , of the order 10^{18} Ampère (e.g. Blandford 1990; Camenzind 1990) which can be carried by the disc-jet system of an AGN, yields an estimate for the pitch for extragalactic jets,

$$\begin{aligned} \frac{\langle P \rangle}{R} &\simeq \frac{1}{R} \frac{R^2 \langle B_z \rangle}{R B_\phi(R)} \\ &\simeq 0.005 \left(\frac{\Phi}{10^{33} \text{ G cm}^2} \right) \left(\frac{I}{10^{18} \text{ A}} \right)^{-1} \left(\frac{R}{0.1 \text{ pc}} \right)^{-1}, \quad (3) \end{aligned}$$

Even if the jets are launched with a large pitch, the pitch necessarily decreases, as the jet propagates and simultaneously becomes wider. Hence most observable jets are expected to possess a small pitch, $P/R \ll 1$. The values relevant for YSOs ($\Phi \simeq 10^{25}$ Gauss cm², $I \simeq 10^{14}$ Ampère, and $R \simeq 10$ AU) lead to similar conclusions.

2.2. Equilibria of magnetized jets

A simple equilibrium which satisfies the scaling above is given by

$$B_\phi = \frac{B_0 r / P_0}{1 + r^2 / P_0^2}, \quad B_z = \frac{B_0}{1 + r^2 / P_0^2}, \quad B_r = 0. \quad (4)$$

This configuration possesses constant pitch, P_0 , which also defines the radial scale length for the magnetic field. The constant pitch model has been applied to jets e.g. by Appl & Camenzind (1993a, 1993b) and Eichler (1993).

Since the precise jet structure is unknown, we consider, in addition to the constant pitch field, equilibria with radially varying pitch. This will provide our results with the required robustness and generality. As a convenient profile we choose

$$P(r) = P_0 \left(1 + C \left(\frac{r}{R} \right)^n \right), \quad (5)$$

where P_0 is the value on the axis, n is a positive integer, and $C > 0$ and $C < 0$ represent equilibria with monotonically increasing and decreasing pitch, respectively. The corresponding equilibrium magnetic field components are calculated numerically. Without loss of generality we restrict ourselves to positive values of P_0 .

As the jet continues to propagate through the interstellar/intergalactic medium, it may undergo a magnetic relaxation process and attain a state of minimum energy (Taylor 1986; Königl & Choudhuri 1985; Appl & Camenzind 1992). Such a relaxation process is observed in laboratory plasmas and leads to magnetic configurations known as reversed field pinches (RFP). Equilibria of this type have previously been considered for CTR (e.g. Bodin & Newton 1980). Despite of $B_z \simeq B_\phi$, they possess favourable stability properties due to the high magnetic shear. A widely used simple model for such an equilibrium is the linear force-free field, $\nabla \times \mathbf{B} = \alpha \mathbf{B}$, with α constant. The Bessel function model (BFM),

$$B_\phi = B_0 J_1(\alpha r), \quad B_z = B_0 J_0(\alpha r) \quad \text{and} \quad B_r = 0, \quad (6)$$

is the solution for cylindrical symmetry. The pitch profile is $P = rJ_0(\alpha r)/J_1(\alpha r)$ with a value $P_0 = 2/\alpha$ on the axis.

3. Stability analysis

A global normal mode stability analysis is performed. The radial displacement, ξ_r , of the fluid elements from their equilibrium positions are of the form, $\xi_r(\mathbf{x}) = \xi_r(r) \exp i(m\phi + kz - \omega t)$, and similarly for the remaining perturbed quantities. The linearized equations can be cast into a system of two first order ODE for $Y \equiv r\xi_r$ and the total perturbed pressure $Z \equiv \delta p_{\text{tot}} = \delta(p + B^2/8\pi)$,

$$AS \frac{dY}{dr} = C_1 Y - rC_2 Z, \quad (7)$$

$$AS \frac{dZ}{dr} = \frac{1}{r} C_3 Y - C_1 Z, \quad (8)$$

with A, S, C_i functions of the equilibrium quantities and the Fourier parameters ω, k, m (Appl & Camenzind 1992).

Jets propagate through a compressible medium of high conductivity. Since one is interested only in instabilities due to the jet itself, radially outgoing decaying waves for large radii define the boundary condition (BC),

$$P \propto H_m^{(1)}(\lambda r) \quad \text{for } r \rightarrow \infty. \quad (9)$$

The $H_m^{(1)}$ are the Hankel functions of the first kind and $\lambda^2 = \omega^2/c_s^2 - k^2$, with c_s the sound speed. The ambient medium has been assumed to be unmagnetized. The perturbed jet is assumed to remain in equilibrium with its surroundings. Regularity on the axis provides the other boundary condition,

$$Y = 0 \quad \text{for } r = 0. \quad (10)$$

The normal mode equations (7) and (8) describe all types of instability that may develop in a cylindrical magnetized outflow, and in the general case it is not possible to clearly separate different types of instabilities. In a setup as simple as described in the previous section, we can attribute the KHI to the vortex sheet at the jet surface. The most dangerous instability is the so-called surface mode, which displaces the entire flow. The body modes give rise to oblique shocks within the jet in the nonlinear regime. The KHI are particularly sensitive to the fast magnetosonic Mach number, and are moderately affected by the magnetic structure. Their growth for the long wavelength instabilities differs at most by a factor of two in the supermagnetosonic regime (Appl & Camenzind 1992). Experience from CTR shows that the behaviour of the CDI strongly depends on the choice of the magnetic profile, and having chosen a constant velocity throughout the jet, we assume that the CDI develops essentially independently from the KHI. CDI of static equilibria are absolute instabilities, i.e. they grow but do not propagate. We further suppose that this is the case also in the rest frame of the jet, and the CDI are therefore simply advected with the flow at the jet velocity. Consequently, no signal can communicate the interior of a supermagnetosonic jet with its surroundings, and we expect that the instabilities behave as if the jet were bounded

by a rigid conducting wall, as long as only CDI are considered. This will be verified numerically in Sect. 5.4. For most calculations of CDI we therefore employ conducting wall boundary conditions,

$$\xi_r(R) = 0. \quad (11)$$

Previous calculations for the BFM with a particular value of α indicate that this is indeed appropriate for CDI provided that the jet velocity is supermagnetosonic (Appl 1996a). We will demonstrate a posteriori in more detail that this choice of boundary condition is justified also for the configurations under consideration. We will also demonstrate that it does not matter whether the return current flows on the jet surface or as a more diffuse current in the ambient medium. Fusion plasmas, on the other hand, are surrounded by a vacuum, with high resistivity and no inertia. These properties are mainly responsible for the destructive behaviour of external modes in CTR. This is one reason that results from fusion research cannot be applied without modification to the case of astrophysical jets. For internal modes that affect mainly an inner plasma region, the boundary conditions are of minor importance, and these instabilities can be supposed to behave in a similar way in jets and fusion plasmas.

A temporal approach is taken: the axial wavenumber k is chosen as real and the differential equations (7,8) formulate an eigenvalue problem for the complex frequency $\omega = \omega_r + i\omega_i$. The imaginary part, $\Gamma \equiv \omega_i$, is the growth rate of a mode specified by k, m . Without loss of generality only the case $k > 0$ is considered in the following. The temporal approach is appropriate for magnetically confined laboratory plasmas and allows an immediate comparison with those results. When calculating eigenvalues, ω , and eigenvectors, ξ_r , in the comoving frame using fixed boundary conditions (11), the unstable modes have purely imaginary eigenvalues, $\omega_r = 0$. In Sect. 5.4 the calculations are performed in a reference frame which is at rest w.r.t. the ambient medium, and radiation boundary conditions (9) are applied. The phase velocity of the instability is then given by ω_r/k .

4. Current-driven instabilities of the linear pinch

A straight cylinder of length $L = 2\pi R_0$ with periodic boundary conditions serves also as a model to study the stability of toroidal configurations with large aspect ratio, R_0/R , designed for thermonuclear fusion, such as the TOKAMAK or the RFP. We have argued in the previous section that CDI are absolute instabilities in the restframe of the magnetized jet, and we therefore very briefly review some of the results obtained for the stability of the static linear pinch that are relevant for our purpose. The most dangerous instability is the $|m| = 1$ current-driven kink instability, due to field-aligned currents, while the axisymmetric pinch modes are stabilized by the absence of a negative pressure gradient.

Resonant surfaces are crucial for the understanding of the CDI. They are magnetic surfaces where the condition $\mathbf{k} \cdot \mathbf{B} = k B_z + (m/r) B_\phi = 0$ holds, or equivalently,

$$kP + m = 0, \quad (12)$$

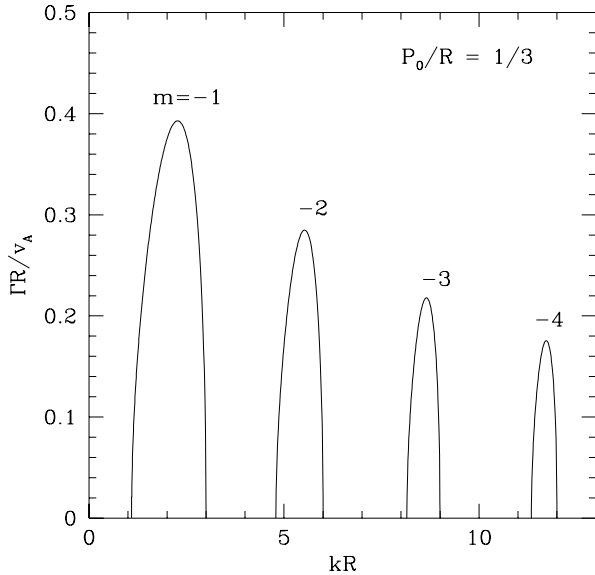


Fig. 1. Constant pitch equilibrium with $P_0/R = \frac{1}{3}$. Growth rate for $m = -1, -2, -3, -4$ (from the left) current-driven instabilities. The instability sets in from the short wavelength side at the resonant condition $k_0 = -m/P_0$.

inside the plasma column, with \mathbf{k} the wavevector of the instability and \mathbf{B} the equilibrium magnetic field. A configuration with resonant surfaces somewhere in the plasma is unstable w.r.t. internal modes, and we will refer to these instabilities also as resonant modes. Consequently, the central core of an infinitely long configuration with radially increasing pitch (where $-m/k > P$) is always unstable for sufficiently long wavelengths, and the modes are generally resonant for an interval in k with $k < k_0$ (k_0 being the limiting wavenumber). A TOKAMAK is also characterized by an increasing q -profile ($q = rB_z/R_0B_\phi$), but the toroidal topology only admits discrete wavenumbers $k = n/R_0$. Consequently, $q_0 > 1$ implies stability w.r.t. $m = -1$ modes (Kadomtsev 1975). Configurations with an increasing pitch profile and central values $P_0/R > 1$ will in the following sometimes be referred as TOKAMAK-like. The most unstable mode in this case is generally resonant.

The perturbed field $\delta\mathbf{B}$ is related to the fluid displacement $\boldsymbol{\xi}$ through Faraday's law, $\delta\mathbf{B} = \nabla \times (\boldsymbol{\xi} \times \mathbf{B})$, which expanded in normal modes yields for the radial component $\delta B_r = i(\mathbf{k} \cdot \mathbf{B}) \xi_r$, i.e. at the resonant surface the radial component of the perturbed magnetic field vanishes. In the case of an increasing pitch profile (and for given k and m) the eigenfunctions ξ_r can, at marginal stability, be approximated by a step function, which is constant within and vanishes outside the resonant surface. The resulting deformation due to a ($m = -1, k$) mode is then a helical distortion of the jet core inside the resonant radius. With increasing growth rate the eigenfunctions become smoother due to inertial effects. The resonances are particularly important for the understanding of the the nonlinear regime of the internal $m = -1$ kink mode of the TOKAMAK (Rosenbluth et al. 1973), where a singular current sheet is forming at

the resonant surface. In the presence of a small non-vanishing resistivity, the current sheet diffuses and drives a magnetic reconnection process.

Not all current-driven instabilities are resonant, however. In particular, a class of fusion devices called *reversed field pinches* (RFP; Bodin & Newton 1980), is characterized by a decreasing pitch profile, which can slightly reverse its sign near the edge. The most unstable (i.e. with the fastest growth) ideal mode (again $m = -1$), is non-resonant from above (Caramana et al. 1983) since $-m/k > P$ everywhere. Unlike the TOKAMAK, no practical necessary and sufficient criteria are available for this type of configuration, and in particular no critical wavenumber where the instability sets in can be given a priori. These instabilities are generally characterized by a somewhat broader and smoother eigenfunction ξ_r than the resonant modes, and they do not vanish at the conducting wall. More important, $\delta B_r \neq 0$ everywhere, and they do not develop singular current sheets in the nonlinear regime (Caramana et al. 1983). For equilibria with monotonically decreasing pitch ($C < 0$ in Eq. (5)) the most unstable mode is non-resonant, similar to the RFP. But note that in spite of its decreasing pitch variation, the dominant kink mode of the unstable BFM configuration can also be a resonant ($m = 1$ in this case) instability, e.g. in the case $\alpha R = 3.83$. The resonant surface, however, is localized in a region of negative pitch.

Finally, magnetic shear, dP/dr , is favourable for the stability of a pinch. Shear and pressure gradient vanish on the axis. This leads to a local stability criterion involving the second derivative of the pitch on the axis (cf. Bodin & Newton 1980),

$$\frac{P}{2} \left. \frac{d^2 P}{dr^2} \right|_{r=0} < \frac{-4}{8 + m^2}. \quad (13)$$

5. Numerical results

Growth rates, eigenfunctions, dispersion relations, etc. are presented for the various linear pinches in the rest frame of the jet using boundary conditions which correspond to a conducting wall, Eq. (11). In the last subsection we a posteriori justify this choice by a comparison with calculations in the rest frame of the ambient medium using radiation boundary conditions.

5.1. The constant pitch field

The constant pitch field, $P = P_0$, is a simple analytic equilibrium with only one free parameter, P_0 . It will turn out that it provides a good model for the instabilities of linear pinches in the regime, $P_0/R \ll 1$, applicable to most MHD jets. The constant pitch field is unstable for all values of P_0 . The resonant condition Eq. (12) only holds for a particular wavenumber, $k = -m/P_0$, which corresponds to the threshold of marginal stability.

We first study the case $P_0/R = \frac{1}{3}$ in some detail before discussing the dependence on the pitch. The growth rate for various azimuthal wavenumbers m is shown in Fig. 1 as a function of the axial wavenumber kR . The instability sets in at the wavenumber where the resonant condition (12) is satisfied. At all other

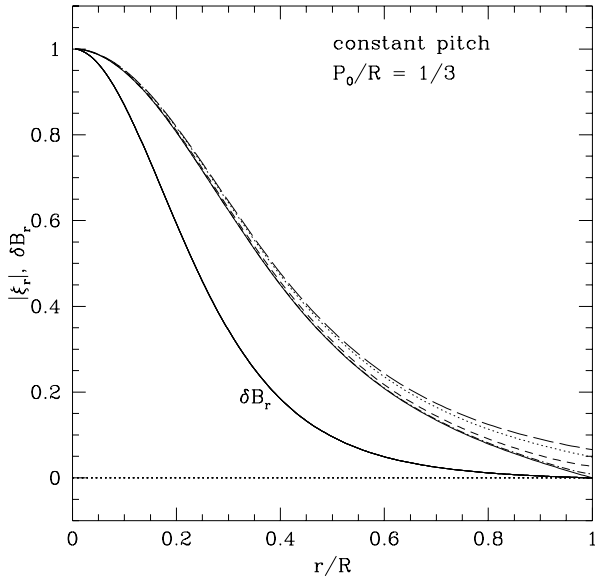


Fig. 2. Eigenfunction of the most unstable kink ($m = -1$) mode for the constant pitch profile with $P_0/R = \frac{1}{3}$. Radial displacement ξ_r (in arbitrary units) as function of the normalized jet radius, for a static equilibrium ($M = 0$) with fixed boundary condition (solid) and radiation boundary condition (dotted), and for a moving equilibrium ($M = 1$) with radiation boundary condition (dashed). Also shown are the cases where no surface current flows on the jet boundary, for $M = 0$ (long-dashed) and $M = 1$ (dash-dotted), using fixed boundary condition at $r = 2R$. In addition, δB_r is shown for the static equilibrium with fixed boundary condition. The corresponding growth rates and wavenumbers are shown in Table 1.

unstable wavelengths the mode is non-resonant. The maximum growth rate (at $kR = k_{\max}R = 2.27$ for the $m = -1$ mode with $P_0/R = \frac{1}{3}$) decreases for increasing azimuthal wavenumber. The non-axisymmetric $m = -1$ kink mode is the most rapidly growing instability, while the $m = 1$ mode is stable in this case. For the rest of the paper we will restrict ourselves to the $|m| = 1$ modes. The solid line in Fig. 2 displays the eigenvector, i.e. the radial displacement ξ_r of the fluid elements and the radial component of the perturbed magnetic field, δB_r , for the most unstable case.

In Fig. 3 the maximum growth rate of the first non-axisymmetric ($m = -1$) mode is displayed as a function of the inverse pitch, $(P_0/R)^{-1}$. Two different regimes can be identified with a transition at $P_0 \simeq R$ and $\Gamma_{\max} \simeq v_A/R$. The large pitch is represented on the left of the diagram, where the magnetic field is dominantly longitudinal. This is the regime where most fusion devices such as the TOKAMAK operate. Growth rates in this limit have been calculated by Goedbloed & Hagebeuk (1972). In this regime the growth rate Γ_{\max} strongly increases with decreasing pitch, $\Gamma_{\max}R/v_A \simeq 0.136 (P_0/R)^{-3}$. For $P_0/R < 1$ a diffuse electrical current is distributed over the entire jet diameter, and the growth of the instability becomes sensitive to the detailed pitch profile. For a dominantly azimuthal field, $P_0/R \ll 1$, as it is likely to be the case for many jets, the growth rate increases only linearly with decreasing pitch. For small values of the pitch the electric current flows

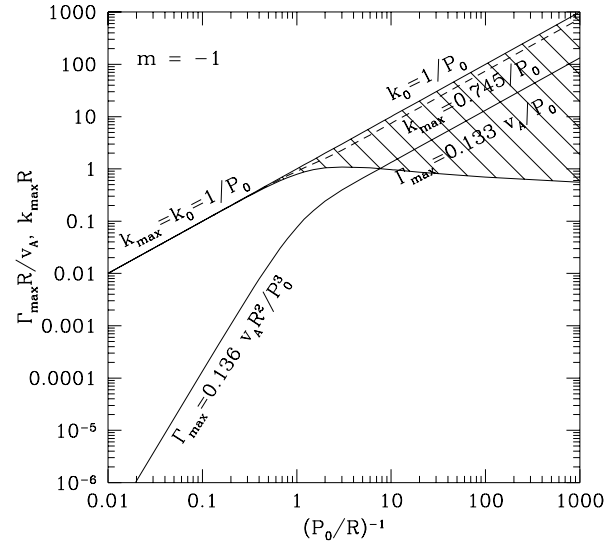


Fig. 3. Maximum growth rate $\Gamma_{\max}R/v_A$ (solid) and most unstable wavenumber $k_{\max}R$ (short-dashed) of the $m = -1$ kink for an equilibrium with constant pitch as a function of $(P_0/R)^{-1}$ with fixed BC. The hatched area covers the range of unstable wavenumbers.

only within a radius of the order P_0 , and the growth rate scales with the Alfvén crossing time for the current-carrying core, $\Gamma_{\max} = 0.133 v_A/P_0$.

The wavenumber, k_0 , where the kink instability sets in, is given by the resonant condition (12), $k_0 = 1/P_0$. For small pitch the wavenumber of the most unstable mode is $k_{\max} = 0.745/P_0$, or equivalently, the wavelength $\lambda_{\max} = 8.43P_0$ (dashed line in Fig. 3), which is of the order of the circumference of the current-carrying core. The instability affects mainly the innermost region of the plasma column. The shape of the dispersion relation, $\Gamma(k)$, remains similar to that of the example with $P_0/R = \frac{1}{3}$ (Figs. 1 and 6), where the growth rates and wavenumbers change according to Fig. 3. The interval of unstable wavenumbers (indicated by the hatched area) becomes larger for decreasing pitch, destabilizing modes over a wide range of wavelengths. For large pitch equilibria, on the other hand, this interval becomes very narrow, and $k_{\max} \simeq k_0 = 1/P_0$, or expressed as a wavelength, $\lambda_{\max} \simeq 2\pi P_0$, for the kink. Hence, in this regime a single mode is destabilized.

5.2. The variable pitch field

The constant pitch field may be considered as a special case, since the unstable modes do not contain resonant surfaces within the plasma. We therefore extend our studies to equilibria with radially varying pitch, considering both monotonically increasing and decreasing pitch profiles. The results of this subsection may give an indication whether the behaviour found from the constant pitch fields is representative of the regime $P_0/R < 1$, and therefore of magnetized jets. We will restrict ourselves to the case of the $m = -1$ kink mode, since it is the most unstable.

Unlike the constant pitch case the resonance condition (12) for increasing pitch is satisfied for an interval in k , which

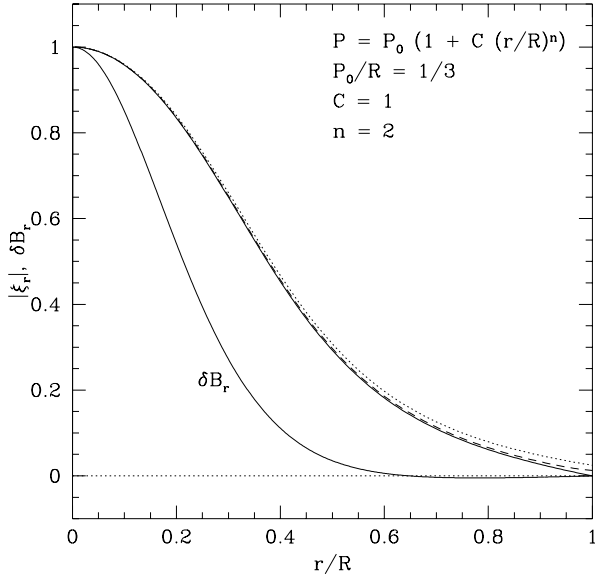


Fig. 4. Eigenfunction of the most unstable kink ($m = -1$) mode for increasing pitch with $P_0/R = \frac{1}{3}$, $C = 1$, $n = 2$. Radial displacement ξ_r (in arbitrary units) as function of normalized jet radius r/R , for static equilibrium ($M = 0$) with fixed boundary condition (solid) and radiation boundary condition (dotted) and for moving equilibrium ($M = 1$) with radiation boundary condition (dashed). In addition, δB_r is shown for the static equilibrium with fixed boundary condition. See Table 1 for growth rates and wavenumbers.

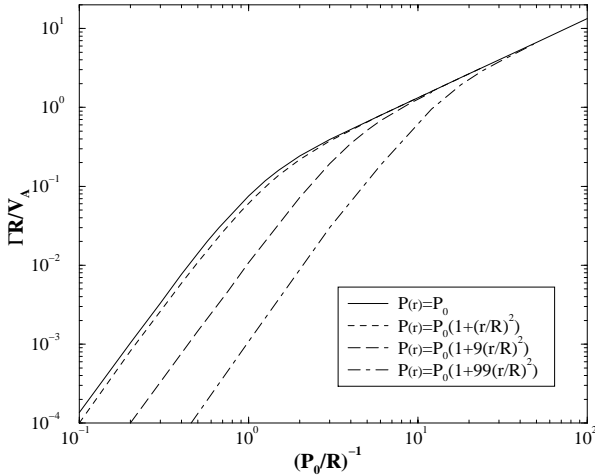


Fig. 5. Maximum growth rate $\Gamma_{\max} R/v_A$ of the $m = -1$ kink as a function of the central pitch $(P_0/R)^{-1}$ for a parabolically increasing ($n = 2$) pitch profile with $C = 1$ (short-dashed), $C = 9$ (long-dashed), $C = 99$ (dash-dotted), and the constant pitch (solid) for comparison.

is determined by the pitch ratio between the boundary and the axis, P_R/P_0 . All modes having a wavenumber k with $-m/P_R \leq k \leq -m/P_0$ are resonant, and for every radius there exists a wavenumber for which the corresponding magnetic surface is resonant. We consider $m = -1$ kink instabilities of equilibria with varying pitch, Eq. (5), where $C > 0$. Fig. 4 shows the radial displacement ξ_r of the most unstable $m = -1$ kink instability for an equilibrium with a parabolic pitch pro-

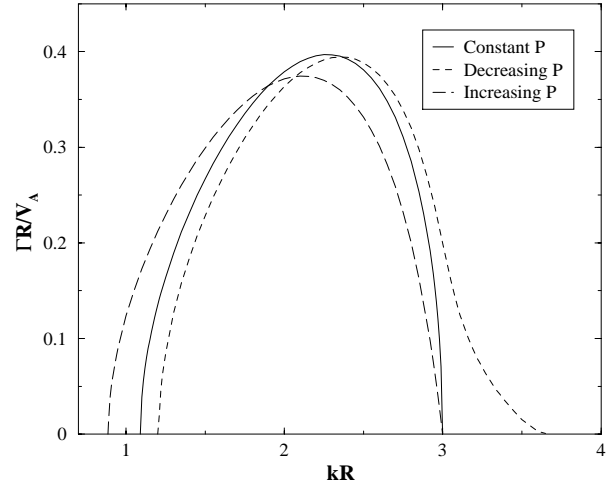


Fig. 6. Growth rate of the $m = -1$ mode as a function of the wavenumber for an equilibrium with (a) constant pitch (solid), (b) an increasing pitch ($C = 1$, $n = 2$; long dashed), and (c) a decreasing pitch ($C = -0.5$, $n = 2$; short dashed) profile. The central pitch is $P_0/R = \frac{1}{3}$ in all three cases. Resonant modes are those with (a) $kR = 3$, (b) $1.5 < kR < 3$, and (c) $kR > 3$.

file ($n = 2$) with the same central pitch value, $P_0/R = \frac{1}{3}$, as before. Comparison with Fig. 2 shows that though the character of the mode has changed from nonresonant to resonant, the radial displacement is only little affected. The distinction plays an important role for the nonlinear evolution of the instability, however (Lery et al. 2000). As in the constant pitch case the instability sets in at $k_0 = 1/P_0$, but now the unstable modes (long-ward) close to the marginal stability threshold become resonant (see long-dashed line in Fig. 6). This implies that the resonant modes cover the interval $1.5 < kR < 3$, including the most unstable mode at $k_{\max} R = 2.11$. Calculations with an exponent $n = 4$ yield very similar results. Fig. 5 shows the maximum growth rate as a function of the central pitch value for several equilibria with quadratically increasing pitch. The configurations with strongly increasing pitch profile ($C = 9$ and $C = 99$) have smaller growth rates for the same central pitch, i.e. a high ratio P_R/P_0 , or equivalently, a high shear dP/dr reduces the growth rate. For small pitch, the maximum growth rate approaches closely the values of the constant pitch field, independently of the equilibrium pitch profile and regardless the different nature of the mode. The same relation holds for the most unstable wavenumber as in the constant pitch case, $k_{\max} = 0.745/P_0$. (This is not displayed in Fig. 5, but see in Fig. 6 that even for $P_0/R = \frac{1}{3}$ the maxima for the constant and increasing pitch with $C = 1$ are close to each other.) For small values of the central pitch the equilibrium (1) yields an electrical current which is concentrated near the axis (unless very extreme pitch variations are considered), where the pitch becomes constant to first order since $P \propto r^2$. Consequently, the instability properties depend essentially on P_0 and are not very sensitive to the profile $P(r)$ in this case. The most unstable mode is resonant when it falls into the k -interval defined by the

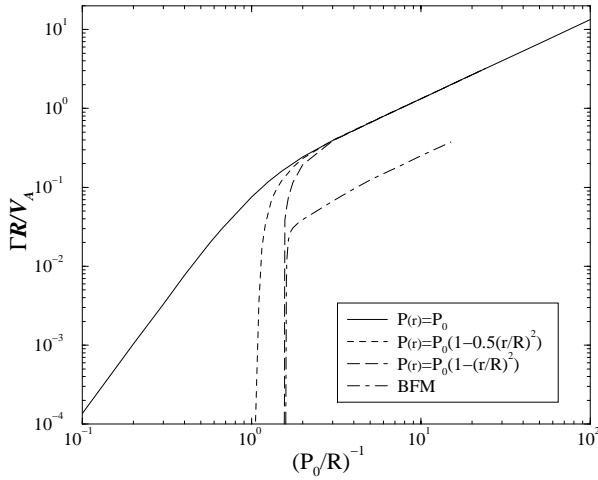


Fig. 7. Maximum growth rate $\Gamma_{\max}R/v_A$ of the $m = -1$ kink as a function of the central pitch P_0/R for a parabolically decreasing ($n = 2$) pitch profile for $C = -1/2$ (short-dashed), $C = -1$ (long-dashed), and the $m = 1$ mode for a linear force-free field (dash-dotted). The $m = -1$ constant pitch (solid) case is displayed for comparison.

resonant condition, i.e. if $P_R/P_0 > 1.326$, and non-resonant otherwise.

The decreasing pitch profiles studied are of the form of Eq. (5), with $C < 0$. The interval for resonant modes is given by $-m/P_0 \leq k \leq -m/P_R$. In the same line of reasoning as above, the resonant modes are now located to the right, i.e. at wavenumbers larger than $k_0 = -m/P_0$. Consequently, instead of the sharp cutoff and stabilization at k_0 , as it is the case for the constant pitch and the monotonically increasing equilibrium, the range of instability is extended towards shorter wavelengths (Fig. 6, short-dashed line). The unstable modes with $k_0R > 3$ are resonant, their growth rate, however, is small. Otherwise the dispersion relation is very similar to the previous cases. Fig. 7 shows the maximum growth rate for equilibria with monotonically decreasing pitch as a function of the central value P_0/R . As it is well known from fusion research, for large pitch the stability behaviour is very sensitive to the profile chosen, and a stabilization is observed for sufficiently large pitch on the axis, corresponding to condition (13). In the small pitch regime, however, the results are essentially indistinguishable from the constant pitch case.

5.3. The linear force-free field

For comparison we consider now the linear force-free field. While the constant-pitch field provided an upper limit for the growth rate, we expect the linear force-free field to represent the lower limit, being a configuration of minimum energy. The CDI for such an equilibrium has been studied for a particular value of $\alpha = 3.83 R$ (Appl 1996a), which has been motivated mainly by the requirement of having a net zero current. The growth rate for the most unstable ($m = 1$) mode, which was resonant in this case, was comparatively low with $\Gamma_{\max} = 0.034 v_A/R$ at $k_{\max}R = 0.7$. We now abandon this restriction and calculate

Table 1. Wavenumber k_{\max} , growth rate Γ_{\max} , and phase velocity v_{ph} of the instability with largest growth rate for equilibria EQ with central pitch $P_0/R = \frac{1}{3}$ and (a) increasing profile ($C = 1$ and $n = 2$) and (b) for constant pitch $P_0/R = \frac{1}{3}$. Radiation (rad) and fixed (fix) boundary conditions at radius r have been applied for various fast Alfvén Mach numbers $M = v/v_A$. In the last two cases the magnetic field extends to $r = 2R$, and the jet surface does not carry a current sheet. The jet velocity is zero for $r > R$ in all cases. The last column refers to the figure displaying the eigenfunction.

EQ	BC	r/R	M	v_{ph}/v_A	$k_{\max}R$	$\Gamma_{\max}R/v_A$	ξ_r in Fig.
a	rad	1	0	0	2.10	0.377	4 (dotted)
a	rad	1	1	1.00	2.11	0.375	4 (dashed)
a	rad	1	3	3.00	2.11	0.375	–
a	fix	1	0	0	2.11	0.375	4 (solid)
b	rad	1	0	0	2.24	0.398	2 (dotted)
b	rad	1	1	1.00	2.26	0.394	2 (dashed)
b	rad	1	3	3.00	2.27	0.393	–
b	rad	2	0	0	2.22	0.403	–
b	rad	2	1	1.00	2.27	0.393	–
b	rad	2	3	3.00	2.27	0.393	–
b	fix	1	0	0	2.27	0.393	2 (solid)
b	fix	2	0	0	2.24	0.399	2 (long-dashed)
b	fix	2	1	1.00	2.27	0.393	2 (dash-dotted)

growth rates for a range in α , corresponding to a central pitch value of $P_0 = 2/\alpha$. It should be noted, however, that unlike the previous equilibria, the BFM is not characterized by a pitch profile with fixed radial dependence, where simply the central value is modified. The profile possesses a varying number of zeroes and poles, depending on the value of α , and consequently on P_0 . The dash-dotted line in Fig. 7 shows that indeed the linear force-free field possesses growth rates nearly an order of magnitude smaller, for the same central pitch value. For numerical reasons we only give results for $P_0/R \gtrsim 0.06$.

5.4. The internal character of the CDI

Growth rates and wavenumbers presented so far have been calculated using fixed boundary conditions. In this subsection we verify numerically whether these boundary conditions are appropriate for current-driven instabilities in jets. Studying the eigenvalue problem Eqs. (7) and (8) with the (correct) radiation boundary conditions we demonstrate that for superalfvénic jet velocities, the current-driven instabilities behave as absolute instabilities in the rest frame of a jet surrounded by a rigid conducting wall. For the particular example of the linear force-free field it has been shown previously (Appl 1996a) that $\Gamma(k)$ were practically identical for the jet and the static configuration bounded by a conducting wall, in particular for supermagnetosonic velocities. For a resonant mode the instability affects mainly the region interior to the $\mathbf{k} \cdot \mathbf{B} = 0$ surface. This makes it plausible that the boundary has only little influence on the mode. One may suspect, however, that non-resonant instabilities are much more affected by the choice of boundary conditions. We there-

fore chose representatives of resonant and non-resonant modes. As examples we take an equilibrium with increasing pitch, with $P_0/R = \frac{1}{3}$, $C = 1$, and $n = 2$, and a constant pitch configuration with $P_0/R = \frac{1}{3}$ and compare the properties of the mode with the largest growth rate for various Mach numbers and boundary conditions (Table 1). The former is a resonant mode, while in the constant pitch case the mode is non-resonant. We applied rigid wall boundary conditions at $r = R$ and radiation boundary conditions both at $r = R$ and $r > R$. For the latter case calculations were performed with $r = 1.01, 2, 3$, which all produce the same results. We therefore only present those corresponding to $r = 2R$. Table 1 shows that their phase velocity in a reference frame where the ambient medium is at rest, $v_{\text{ph}} = \omega_r/k$, is equal to the jet velocity, as indicated by the Mach number, $M = v/v_A$. CDI are therefore absolute instabilities in the rest frame of the jet. We further note that the most unstable wavenumber, k_{max} , as well as the maximum growth rate, Γ_{max} , are only little affected by the jet velocity, and for high Mach number they become indistinguishable from a jet with rigid boundary. The same is true for the eigenfunctions (Figs. 2 and 4).

A comparison over a much wider range in Mach numbers and wavenumbers, shown in Fig. 8 for the constant pitch case, confirms that in fact the most unstable mode is unaffected by the choice of boundary conditions, even at relatively low Mach number. With radiation BC the unstable wavenumbers extend to larger wavelengths, and for Mach numbers, $0 < M \lesssim 1.5$ the CDI is modified by the velocity gradient (not displayed). We take the results of this subsection as justification that current-driven instabilities in jets are correctly modeled by boundary conditions describing a perfectly conducting rigid wall.

Both the conducting wall BC and the radiation BC used so far correspond to a return current that flows on the surface of the jet. The jet is therefore confined by external pressure. In order to study whether the results are sensitive to the surface current sheet, we compare them to a constant pitch equilibrium where the magnetic field extends to $r = 2R$, while the jet, defined by the plasma motion, is restricted to $r < R$. The results remain unaffected (see Table 1 and Fig. 2), and come even closer to the case with fixed BC at $r = R$. For $M = 1$ the eigenfunction possesses a kink at the jet boundary at $r = R$, and ξ_r remains very small at $r > R$ (not visible in Fig. 2).

6. Discussion

Global current-driven instabilities of magnetized jets are studied in the linear regime. For this purpose a normal mode analysis has been performed for force-free screw pinches. The stability of such equilibria is conveniently discussed in terms of the magnetic pitch, $P = rB_z/B_\phi$. Various magnetic pitch profiles have been probed, in particular equilibria with constant, and both radially increasing and decreasing pitch, and allow us to draw conclusions about MHD jets in general.

The stability properties can be discussed in terms of a single parameter, the pitch value on the axis, P_0 . There exist two clearly separated regimes, with a transition depending on the profile.

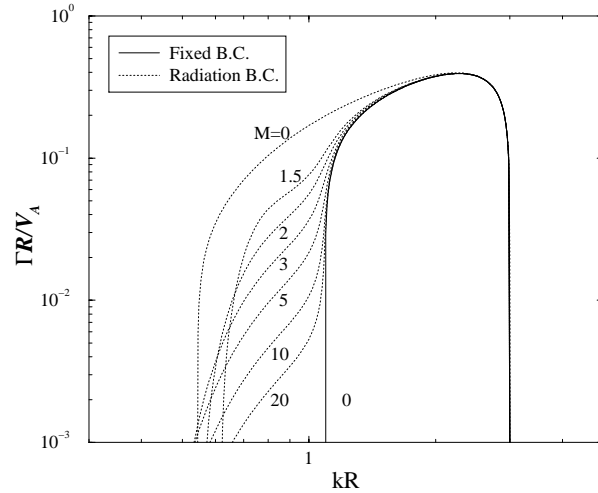


Fig. 8. Growth rate for the $m = -1$ mode for the constant pitch profile with $P_0/R = \frac{1}{3}$ for various Mach numbers (indicated by the labels) and radiation boundary condition (dotted) and for a static equilibrium ($M = 0$) with fixed boundary condition (solid).

The transition occurs at $P_0/R \simeq 1$ for equilibria with moderate shear. The high-pitch regime, $P_0/R > 1$, where the majority of fusion machines operate, has been extensively studied in the literature. It is characterized by a strong longitudinal field, and the stability properties are highly sensitive to the particular pitch profile. The constant pitch model exhibits CDI with the largest growth rate among the equilibria studied. The configuration with increasing pitch, i.e. a TOKAMAK-like pinch, shows, for small and moderate shear, a behaviour very similar to the constant pitch case, while equilibria with a decreasing pitch become stabilized at sufficiently large central pitch. Most magnetized jets are likely to possess a dominantly azimuthal field, and consequently a small pitch, $P_0/R < 1$. With decreasing P_0/R the current becomes more and more concentrated on the axis, within a radius of the order P_0 , and the growth time and the wavelengths of the instabilities become correspondingly shorter, scaling linearly with P_0/R as $t_g = 7.52 P_0/v_A$ and $\lambda_{\text{max}} = 8.43 P_0$, respectively. The results of Figs. 3, 5, and 7 indicate that, in this regime, both the growth rate and the wavenumber where the instability grows fastest, k_{max} , are insensitive to the particular pitch profile. Therefore, the constant pitch case yields very good estimates for the growth and the wavelength of current-driven instabilities in magnetized jets, and it provides a robust and simple model for the study the linear evolution of the CDI in the regime $P_0/R \ll 1$. The growth rate becomes inversely proportional to the pitch, $\Gamma_{\text{max}}R/v_A = 0.133 (P_0/R)^{-1}$, while in the large pitch regime it is much more sensitive, e.g. for the constant pitch equilibrium the growth rate depends on the third power of the pitch, $\Gamma_{\text{max}}R/v_A = 0.136 (P_0/R)^{-3}$. For comparison we presented results for a linear force-free field. For central pitch $P_0 < 2/\alpha = 0.63$ the cylindrically symmetric linear force-free becomes unstable w.r.t. non-axisymmetric perturbations. Being a minimum energy configuration, it is not astonishing that this kind of equilibrium possesses particularly favourable stability properties, with growth rates that are nearly an order of magni-

tude smaller than for the other equilibria. The wavelength of the most unstable mode is larger, too, than for the other equilibria studied. The constant-pitch and the linear force-free field represent extreme situations, corresponding to the most and least unstable configurations, respectively.

For small pitch the stability properties become essentially independent of the details of the pitch profile. While the nature of the instability (resonant or not) does not affect the growth rate and the axial wavelength of the most unstable mode, an important difference consists in the radial component of the perturbed magnetic field. The latter can vanish at some resonant radius only for an increasing pitch profile. Since it is well known from the non-linear evolution of the internal kink mode in TOKAMAKs that a current sheet forms at the resonant radius, we have studied its non-linear evolution in the small pitch regime by means of a time-dependent 3D MHD code (Lery et al. 2000).

In general, both current-driven and Kelvin-Helmholtz instabilities are present in the kind of jet models considered, and in the general case it is not possible to classify them unambiguously. To this end we have studied jet models which are particularly simple, and which are characterized by a constant density and velocity. In this approximation the CDI and the KHI can be identified for supermagnetosonic jets by comparing them to the static and the current-free counterparts, respectively. A velocity shear would lead to a more complicated coupling between the KHI and the CDI. Instabilities with wavelengths which are large compared to the radial scale of the shear behave essentially as in the case of a vortex sheet. Furthermore, in configurations with small pitch the electric current, and consequently also the instability is concentrated in the vicinity of the axis. In this case a velocity shear which is likely to be largest near the jet boundary does not affect the instability very much either. Current-driven instabilities can then be studied in the rest frame of the jet plasma, and the motion only enters through appropriately chosen boundary condition.

The normal modes of static MHD plasmas can be classified according to their properties as (slow and fast) magnetoacoustic and Alfvén modes. These are “wave-like” disturbances for which a super-fast-magnetosonic shear layer essentially becomes impermeable. The situation is different for the Kelvin-Helmholtz surface modes. Here it is the (supersonic) velocity itself which by virtue of its inertia deforms the boundary of the jet. We argue that for supermagnetosonic flows CDI develop essentially as if the jet were surrounded by a rigid wall. We examined the properties of current-driven instabilities of jets with different Mach numbers using radiation boundary conditions which are most appropriate for this purpose. We find that in fact the CDI is an instability in the rest frame of the jet, and for high Mach numbers the dispersion relation and the eigenfunctions become indistinguishable from the static case, i.e. the jet boundary is not radially displaced in the linear regime. At low Mach number the dispersion relation shows a more complicated behaviour, due to the interaction with the velocity shear. In this regime it becomes difficult to disentangle the different types of instabilities. The maximum growth rate and the most

unstable wavenumber, however, remain nearly unaltered, even for vanishing velocity. This was analyzed for the constant pitch field and a configuration with radially increasing pitch, i.e. for a non-resonant and a resonant mode, respectively (Table 1). It confirms that CDI in jets are instabilities which grow in the restframe of the jet, and that it is justified to study them using fixed boundary conditions, as was done in most of the numerical calculations.

The jet configurations analyzed generally possess a net electrical current. The return current either flows back on the surface of the jet, or as a more diffuse current distributed over a larger region in the ambient medium. A comparison showed that the results are not much affected by this choice. The perturbation, ξ_r , in both cases essentially remains confined to the jet interior, and the ambient medium has very little influence on the CDI. Fixed BC or radiation BC in combination with an unmagnetized ambient medium at $r > R$ imply that the jet is confined by ambient pressure. An azimuthal field in the ambient medium, as it has been assumed in another calculation, corresponds to a magnetically confined jet. If we suppose that these results hold for the general case, this indicates that the growth of current-driven instabilities in jets is independent of the confinement mechanism.

7. Astrophysical consequences

We have studied the kink instability in magnetized jets. It has been found that the constant pitch model provides good estimates for growth rates and wavelengths in the small pitch regime. The previous results will be applied to VLBI jets from AGN, which are characterized by relativistic velocities. The linear evolution of the instability is described by a non-relativistic treatment in the rest-frame of the bulk flow, if the additional inertia due to the magnetic field and the displacement current (Begelman 1998) is neglected. The opposite limit, where the rest mass has been assumed to be negligible compared to the electromagnetic energy, has been considered by Istomin & Pariev (1994, 1996), and Lyubarskii (1999). The Lorentz factor $\gamma = (1 - v^2/c^2)^{-1/2}$, as well as the forces due to the electric field, $\rho_e \mathbf{E}$ are second order in the perturbed quantities and do not contribute in a linear analysis.

The equilibrium magnetic field is related to the jet velocity by the ideal MHD condition, $\mathbf{v} = (\eta/\gamma n) \mathbf{B}' + r \Omega_* \mathbf{e}_\phi$, where now B'_z and B'_ϕ are the laboratory fields, measured in a system at rest in the external medium, Ω_* is the angular velocity of the footpoint where the poloidal field lines are anchored, η is the mass flux per magnetic flux, and n the proper particle density. For large radii the rotation of the plasma can be neglected, and eliminating $(\eta/\gamma n)$ from the MHD condition we obtain for the jet velocity $v \simeq r \Omega_* B'_z / B'_\phi$. The corresponding rest frame fields are B_z and B_ϕ/γ , respectively, and the relation between the jet velocity and the magnetic pitch in the rest frame becomes $\gamma v = P \Omega_*$ (Appl & Camenzind 1993b). Choosing for Ω_* the Keplerian rotation at the marginally stable orbit, $r_* = 6r_g$, of a Schwarzschild black hole ($r_g = GM/c^2$), we obtain $P_0/R \simeq 20 (\gamma v/c) (R/r_g)^{-1}$. Among the observable

jets only narrow, powerful objects such as quasars can therefore be expected to have a dominantly longitudinal magnetic field with large pitch, while less powerful jets (e.g. from BL Lac objects), correspond to very small values of the pitch. Even if at the base jets have $P/R \simeq 1$, as they open up and become wider, their pitch necessarily decreases to small values. The current-driven instabilities do not propagate in the rest frame of the plasma, but are advected with the relativistic jet velocity. The jet propagates a distance $l_g = vt'_g = \gamma vt_g$ during an e-folding time, where t'_g is the growth time in the observer's frame. We find for the distance propagated during one e-folding time, $l_g \simeq 150 (\gamma v/c)^2 (c/v_A) r_g$, or putting numbers appropriate for the VLBI jets,

$$\frac{l_g}{R} = 7.52 \frac{P_0}{R} \frac{\gamma v}{v_A} \simeq 0.0752 \left(\frac{\gamma v}{c}\right)^2 \left(\frac{v_A}{c}\right)^{-1} \left(\frac{R}{0.1 \text{ pc}}\right)^{-1} \left(\frac{M}{10^9 M_\odot}\right). \quad (14)$$

According to this estimate only in powerful relativistic jets from massive objects the magnetic structure can survive over distances of many jet radii. The growth rate possesses a maximum at a well defined wavelength, and the instability consists of a non-axisymmetric perturbation advected with the bulk flow. We can speculate that dissipative processes resulting from the kink instability are responsible for the necessary in situ acceleration of synchrotron electrons, or are related to the formation of the VLBI knots, which apparently are non-axisymmetric features within the flow channel (Zensus et al. 1995). Observable features in large scale jets, such as the helical filaments in the jets of M87 (Biretta 1996) and 3C273 (Bahcall et al. 1995) are, however, unlikely to be due to kink instabilities of equilibria such as the constant pitch field. The simple scaling arguments preceding Eq. (3) indicate that, when the jet opens to radii of the order of several pc, the pitch becomes very small, and consequently, the fast kink mode will alter the magnetic structure long before the plasma has reached the distances where these filaments are observed. We conclude that, if not stabilized nonlinearly, the magnetic field configurations, as they result from the collimation zone, will not survive unaltered out to large distances. The instability would continue to operate until a large fraction of the electric current is dissipated, and the pitch has increased to a much smaller value. This does not mean, however, that the jet is disrupted (see below). Unstable modes are excited over a large wavelength regime, where the dominant mode possesses a wavelength much smaller than the jet radius. This may give rise to turbulent dissipation. For magnetically confined outflows this can result in a loss of collimation due to current dissipation. Such a jet would continuously become wider and eventually become confined by the pressure of the ambient medium. The internal structure of the jet is expected to undergo a magnetic relaxation process (Taylor 1986) and settle into a minimum energy configuration, which for sufficiently wide jets possesses a non-axisymmetric contribution (Königl & Choudhuri 1985). The helical filaments may then be kink instabilities triggering the transition to the non-axisymmetric minimum energy state (Appl 1996b), given that the growth rate for the linear force-

free field are about an order of magnitude smaller than for the other examples.

Königl & Choudhuri (1985) argued that supersonic motion would suppress ripples at the interface of the jet, and that therefore the relaxation of the magnetic field would proceed as if the jet were bounded by a rigid wall. Eichler (1993) criticized that according to this line of reasoning the Kelvin-Helmholtz instability would not develop either. Our results lead us to conclude that the CDI in jets are internal modes, which do not deform the surface. If this remains true in the nonlinear regime, these jets will not be disrupted by external kink instabilities, as has been argued by Eichler (1993) and Spruit et al. (1997). However, the internal kink appears to behave essentially the same way, whether the jet is confined by any external pressure or by the hoop stresses of its own magnetic field. This is likely to lead to the dissipation of most of the electric current. In this case magnetic confinement would not be maintained over very large distances. The same mechanism may also put a limit on magnetic collimation at the base by magnetic fields alone.

For jets with $B_\phi > B_z$ the growth rate of the CDI is only a fraction of the Alfvén crossing time and therefore generally much shorter than for the KHI. Since in supermagnetosonic jets the CDI does not involve the jet boundary, and the kinetic energy dominates the magnetic energy we have argued that the CDI will not destroy such jets, but lead to dissipation of the electric current, thereby altering the magnetic structure. The gross dynamics of a pressure confined jet may then be governed by the KHI of a magnetized jet with a modified magnetic configuration. The KHI of MHD jets has been shown not to be too sensitive to the details of the magnetic profile, if instead of the hydrodynamic Mach number the fast magnetosonic Mach number is taken (Appl & Camenzind 1992). It can therefore be misleading to conclude on the fate of the jet by considering growth rates alone. Relativistic motion is favourable for stability in both cases. High Lorentz factors reduce the growth of CDI kinematically through time dilatation, and the KHI are in addition stabilised dynamically by an enhanced inertia.

The results of this paper, as well as most consequences, also apply to the case of jets from young stellar objects. Due to their non-relativistic velocities the CDI in jets from YSO are expected to grow even more rapidly. Dissipation of the electrical current may provide the necessary heating to explain the observed line emission. The regularly spaced knots (e.g. Zinnecker & McCaughrean 1997) however appear to be on the jet axis, and are therefore not likely to be due to non-axisymmetric CDI as they are discussed here. Unlike in extragalactic jets, thermal effects and radiative losses are dynamically important. Jet models taking into account typical conditions at the jet base are characterized by large negative pressure gradients, which can destabilize axisymmetric modes (Lery et al. 1998, 1999).

We have discussed and presented results for highly idealized jet models. Real jets certainly possess a velocity and density gradient, which makes a similar analysis impractical and less clear-cut. Since our results are pretty robust in the regime relevant to jets, they provide a useful guideline for the properties of current-driven instabilities in jets.

Acknowledgements. We are grateful to J. Heyvaerts for stimulating discussions. S.A. acknowledges support from the Deutsche Forschungsgemeinschaft (SFB 359), and T.L. was partly supported by an operating grant from NSERC of Canada.

References

- Appl S., 1996a, *A&A* 314, 995
 Appl S., 1996b, In: Hardee P.E., Bridle A.H., Zensus J.A. (eds.) *Energy Transport in Radio Galaxies and Quasars*. ASP Conference Series Vol. 100, NRAO (Greenbank), p. 129
 Appl S., Camenzind C., 1992, *A&A* 256, 354
 Appl S., Camenzind M., 1993a, *A&A* 270, 71
 Appl S., Camenzind M., 1993b, *A&A* 274, 699
 Bahcall J.N., Kirhakos S., Schneider D.P., et al., 1995, *ApJ* 452, L91-L93
 Bateman G., 1978, *MHD Instabilities*. MIT Press, Cambridge
 Begelman M.C., 1998, *ApJ* 493, 291
 Begelman M.C., Blandford R.D., Rees M.J., 1984, *Rev. Mod. Phys.* 56, 255
 Biretta J.A., 1996, In: Hardee P.E., Bridle A.H., Zensus J.A. (eds.) *Energy Transport in Radio Galaxies and Quasars*. ASP Conference Series Vol. 100, NRAO (Greenbank), p. 187
 Blandford R.D., Payne D.G., 1982, *MNRAS* 199, 883
 Blandford R.D., 1990, In: Blandford R., Netzer H., Woltjer L. (eds.) *Active Galactic Nuclei*. Saas-Fee Lecture Notes, Springer
 Bodin H.A.B., Newton A.A., 1980, *Nuclear Fusion* 20, 1255
 Camenzind C., 1990, In: Klare G. (ed.) *Reviews of Modern Astronomy* 3, Springer, Berlin
 Caramana E.J., Nebel R.A., Schnack D.D., 1983, *Phys. Fluids* 26, 1305
 Eichler D., 1993, *ApJ* 419, 111
 Fendt C., Camenzind M., Appl S., *A&A* 300, 791
 Goedbloed J.P., Hagebeuk H.J.L., 1972, *Phys. Fluids* 15, No. 6, 1090
 Heyvaerts J., Norman C., 1989, *ApJ* 347, 1055
 Istomin Ya.N., Pariev V.I., 1994, *MNRAS* 267, 629
 Istomin Ya.N., Pariev V.I., 1996, *MNRAS* 281, 1
 Kadomtsev B.B., 1975, *Sov. J. Plasma Phys.* 1, 389
 Königl A., Choudhuri A.R., 1985, *ApJ* 289, 173
 Lery T., Baty H., Appl S., 2000, *A&A* in press
 Lery T., Heyvaerts J., Appl S., Norman C.A., 1998, *A&A* 337, 603
 Lery T., Heyvaerts J., Appl S., Norman C.A., 1999, *A&A* 347, 1055
 Lyubarskii Yu.E., 1999, *MNRAS* 308, 1006
 Pearson T.J., 1996, In: Hardee P.E., Bridle A.H., Zensus J.A. (eds.) *Energy Transport in Radio Galaxies and Quasars*. ASP Conference Series Vol. 100, NRAO (Greenbank), p. 97
 Reipurth B., Heathcote S., 1997, In: Reipurth B., Bertout C. (eds.) *Herbig-Haro flows and the birth of low mass stars*. IAU Symposium 182, p. 3
 Rosenbluth M.N., Dagazian R.Y., Rutherford P.H., 1973, *Phys. Fluids* 16, 1894
 Shu F.H., Najita J., Ostriker E., et al., 1994, *ApJ* 429, 781
 Spruit H.C., Foglizzo T., Stehle R., 1997, *MNRAS* 288, 333
 Taylor J.B., 1986, *Rev. Mod. Phys.* 58, 741
 Zensus J.A., Krichbaum T.P., Lobanov A.P., 1995, *Proc. Natl. Acad. Sci. USA* 92, 11348
 Zinnecker H., McCaughrean M., 1997, In: Malbet F., Castets A. (eds.) *Low Mass Star Formation - from Infall to Outflow*. Poster proceedings of IAU Symposium No. 182 on Herbig-Haro Objects and the Birth of Low Mass Stars, p. 198